

- Turkdogan, E. T., R. G. Olsson, and J. V. Vinters, "Pore Characteristics of Carbons," *ibid.*, 545 (1970a).
- Turkdogan, E. T., and J. V. Vinters, "Catalytic Oxidation of Carbon," *ibid.*, 97 (1972).
- Walker, P. L., Jr., R. J. Foresti, and C. C. Wright, "Surface Area Study of Carbon-Carbon Dioxide Reaction," *Ind. Chem. Eng.*, 45, 1703 (1953).
- Walker, P. L., Jr., F. Rusinko, Jr., and E. Raats, "Changes of Macropore Distributions in Carbon Rods Upon Gasification with Carbon Dioxide," *J. Phys. Chem.*, 59, 245 (1955).
- Walker, P. L., Jr., and E. Raats, "Changes in Physical Properties of Graphitized Carbon Rods Upon Gasification with Carbon Dioxide," *ibid.*, 60, 364 (1956).
- Walker, P. L., Jr., F. Rusinko, Jr., and L. G. Austin, "Gas Reactions of Carbon," in *Advance in Catalysis*, Vol. XI, p. 133, Academic Press, New York (1959).
- Wang, S. C., and C. Y. Wen, "Experimental Evaluation of Nonisothermal Solid-Gas Reaction Model," *AIChE J.*, 18, 1231 (1972).
- Wen, C. Y., and S. C. Wang, "Thermal and Diffusional Effects in Non-Catalytic Solid-Gas Reactions," *Ind. Eng. Chem.*, 62, 30 (1970).
- Wen, C. Y., "Noncatalytic Heterogeneous Solid Fluid Reaction Models," *ibid.*, 60, 34 (1968).
- Wicke, E., "Contributions to the Combustion Mechanism of Carbon," in *Fifth Symposium on Combustion*, p. 245, Reinhold, New York (1955).
- Yoshida, K., and D. Kunii, "Gasification of Porous Carbon by Carbon Dioxide," *Chem. Eng. J. (Japan)*, 2, 1170 (1969).

Manuscript received December 23, 1975; revision received July 20 and accepted July 22, 1976.

The Effect of Flow Maldistribution on Conversion in a Catalytic Packed-Bed Reactor

Part I. Analysis

MANOJ CHOUDHARY

JULIAN SZEKELY

and

SOL W. WELLER

Department of Chemical Engineering
State University of New York at Buffalo
Buffalo, New York 14214

Through the statement of the vectorial form of the Ergun equation, combined with a differential component balance, a formulation was developed describing the velocity fields and reactant concentration profiles in an isothermal packed-bed reactor in which the gas flow is nonuniform. This flow maldistribution was caused by both the preferential flow near the wall, inherent in most systems, and by the deliberate arrangement of the solid packing in the bed. The numerical solution of the governing equations showed that a nonuniform flow field had a very strong effect in distorting the concentration isopleths, particularly at intermediate conversion levels.

SCOPE

The quantitative understanding of the effect of non-uniform gas flow on the performance of packed-bed reactors is a problem of considerable practical importance in chemical reaction engineering. It has been suggested that

hot spot formation and temperature excursions may well be associated with or are the direct consequence of non-uniform flow. In recent years, numerous theoretical studies have been made of nonuniform flow in packed-bed reactors (Radestock and Jeschar, 1969, 1970, 1971a, 1971b; Stanek and Szekely, 1972, 1973, 1974), and more recently direct experimental proof has been provided con-

Manoj Choudhary and Julian Szekely are with the Department of Materials Science and Engineering, Massachusetts Institute of Technology, Cambridge, Massachusetts 02139.

cerning the appropriateness of this approach (Szekely and Poveromo, 1975). While this work was motivated by its relevance to chemical reaction engineering, the concepts of nonuniform flow have yet to be applied to the modeling of packed-bed reactors. The purpose of the work to be described in this paper is to develop a mathematical statement of the effect of flow maldistribution on the performance of a catalytic packed-bed reactor. A simple case will be examined where the system

is isothermal and the reaction is of first order. The resultant differential equations are solved numerically, and the parameters for the computation are so chosen to correspond to those used in a subsequent experimental study. Thus, the principal objective of the work is to represent the effect of flow maldistribution on conversion and to allow the comparison of the resultant predictions with experimental measurements, albeit for a simple case.

CONCLUSIONS AND SIGNIFICANCE

Through the statement of the vectorial form of the Ergun equation, combined with a differential component balance, a mathematical formulation was developed describing the velocity fields and reactant concentration profiles in an isothermal packed-bed reactor with flow maldistribution. This flow maldistribution was caused by both the preferential flow near the wall inherent in all systems and by the deliberate nonuniform packing of the system.

The numerical solution of the governing equations indicated that the nonuniform flow field had a very strong effect in distorting the concentration isopleths. As far

as total conversion was concerned, this effect was most pronounced at intermediate conversion levels.

The principal significance of the work is thought to be the fact that it represents the first mathematical statement of the effect of flow maldistribution on the performance of catalytic packed-bed reactors where appropriate kinetic expressions are combined with the vectorial form of the Ergun equation. The parameters in the computation were so selected as to allow ready comparison with measurements.

The predictions based on the model are tested experimentally in Part II of the paper.

In recent years, there has been a growing interest in the role of hot spots and temperature excursions in effecting the malfunctioning of catalytic packed bed reactors (Jaffe, 1976). It has been generally recognized that hot spot formation is associated with flow maldistribution which may then be aggravated with spatially nonuniform temperatures within the system.

Notwithstanding the fact that a flat (uniform) velocity profile is usually assumed to exist in packed-bed reactors, it has been known for a long time that uniform flow does not occur even in uniformly packed beds because of the tendency for preferential flow near the walls (Furnas, 1929). The existence of a higher local void fraction near the wall of packed beds, which is consistent with the ideas of preferential flow, has been demonstrated by Benenati and Brosilow (1962). In general, nonuniform flows in packed beds may occur owing to spatially non-uniform resistance to flow (for example, nonuniform

porosity, laterally distributed temperature, etc.) or owing to the presence of side streams.

Systematic studies of multidimensional flows in packed beds have been described by Radestock and Jeschar (1969, 1970, 1971a, 1971b) and by Stanek and Szekely (1972, 1973, 1974). In essence, these authors expressed the Ergun equation in a vectorial form and then devised various algorithms for the numerical solution of the resultant differential equations. More recently, Szekely and Poveromo (1975) furnished direct experimental proof regarding the appropriateness of this approach.

Notwithstanding the fact that all the above-cited work was motivated by its application to chemical reaction engineering, the actual extension of these ideas to describe chemical reactions in maldistributed beds has not yet been accomplished. The work to be described in the present series of papers was undertaken with the objective of modeling the rate of catalytic reactions in packed-bed reactors where the flow of the reactant gas is nonuniform and then to compare the predictions based on the model with actual measurements.

In order to make the problem tractable, both experimentally and from the computational viewpoint, an essentially thermoneutral system was chosen in the first instance so that the assumption of isothermal behavior was appropriate.

In the present Part I of the paper we shall present the mathematical formulation together with the computed results, while the subsequent Part II will be devoted to the experimental program and to the comparison of the measurements with predictions.

FORMULATION

Let us consider a cylindrical packed-bed reactor of radius R and of height L which may be packed in a spatially nonuniform manner, but with cylindrical sym-

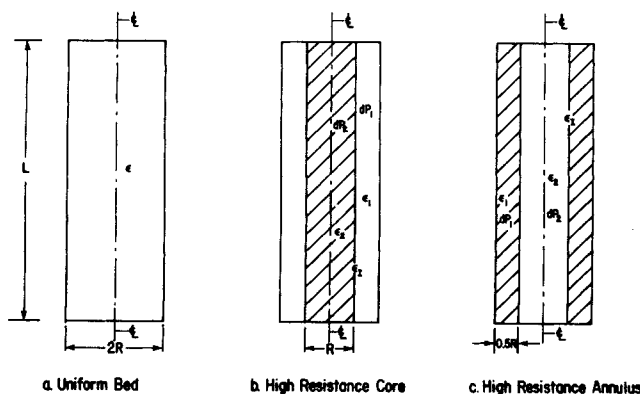


Fig. 1. Packing configurations considered for computation (the shaded area indicates zone of high resistance). a) uniform bed, b) bed with a high resistance central core, c) bed with a high resistance annulus.

metry observed, as sketched in Figure 1. As indicated in the figure, by assigning values to the porosity and the particle size in the shaded and the unshaded regions, the flow resistance of the annular and the core regions may be appropriately defined.

Let us consider, furthermore, that the following simple, heterogeneous, irreversible chemical reaction takes place in the system:



which may be represented in terms of a pseudo homogeneous model. Finally, the reaction is assumed to be thermoneutral so that the system is isothermal throughout.

Within the framework of these assumptions, the problem is readily stated by writing the equations of continuity, motion, and the component balance. For the simple reaction considered there is no change in molarity, so that the component balance and the momentum balance equations are uncoupled.

FLUID FLOW EQUATIONS

Using vector notation, we write the equation of continuity as

$$\nabla \cdot \vec{V}' = 0 \quad (1)$$

Moreover, the vectorial form of the Ergun equation is expressed as

$$\nabla P' = - \vec{V}'(f_1 + f_2 V') \quad (2)$$

where f_1 and f_2 are the Ergun coefficients (Ergun, 1952).

Upon using $\nabla \times$ operator on both sides of Equation (2), we have

$$\nabla \times \vec{V}' - \vec{V}' \times \nabla [\ln(f_1 + f_2 V')] = 0 \quad (3)$$

Upon introducing the following dimensionless parameters

$$a = R/L, \quad V = V'/V_o', \quad r = r'/R, \quad z = z'/L, \quad \xi = f_1/(f_2 V_o') \quad (4)$$

and upon noting the criteria for axial symmetry, we have

$$a \frac{\partial V_r}{\partial z} - \frac{\partial V_z}{\partial r} + \frac{1}{f_2(\xi + V)} \left[a V_r (\xi + V) \frac{\partial f_2}{\partial z} + a V_r f_2 \frac{\partial(\xi + V)}{\partial z} - V_z (\xi + V) \frac{\partial f_2}{\partial r} - V_z f_2 \frac{\partial(\xi + V)}{\partial r} \right] = 0 \quad (5)$$

Upon defining the stream function ψ as

$$V_z = -\frac{1}{r} \frac{\partial \psi}{\partial r}; \quad V_r = \frac{a}{r} \frac{\partial \psi}{\partial z} \quad (6a, b)$$

we may write Equation (5) as

$$\left[\left(\frac{\partial \psi}{\partial z} \right)^2 + \frac{2}{a^2} \left(\frac{\partial \psi}{\partial r} \right)^2 + \frac{\xi V r^2}{a^2} \right] \frac{\partial^2 \psi}{\partial r^2} + \left[2a^2 \left(\frac{\partial \psi}{\partial z} \right)^2 + \left(\frac{\partial \psi}{\partial r} \right)^2 + \xi V r^2 \right] \frac{\partial^2 \psi}{\partial z^2} + \left[\left\{ \left(\frac{\partial \psi}{\partial r} \right)^2 + a^2 \left(\frac{\partial \psi}{\partial z} \right)^2 \right\} \left\{ \frac{1}{a^2} \left(\frac{\partial \ln f_{20}}{\partial r} - \frac{2}{r} \right) \right\} + \frac{1}{a^2} \left\{ -\xi V r + V r^2 \frac{\partial \xi}{\partial r} + \xi V r^2 \frac{\partial \ln f_{20}}{\partial r} \right\} \right] \frac{\partial \psi}{\partial r}$$

$$+ \left[\left\{ \left(\frac{\partial \psi}{\partial r} \right)^2 + a^2 \left(\frac{\partial \psi}{\partial z} \right)^2 \right\} \frac{\partial \ln f_{20}}{\partial z} + \left\{ V r^2 \frac{\partial \xi}{\partial z} + \xi V r^2 \frac{\partial \ln f_{20}}{\partial z} \right\} \right] \frac{\partial \psi}{\partial z} + 2 \frac{\partial \psi}{\partial r} \frac{\partial \psi}{\partial z} \frac{\partial^2 \psi}{\partial r \partial z} = 0 \quad (7)$$

which also satisfies the equation of continuity.

Here

$$f_{20} = \frac{f_2}{f_{2r}} = \frac{1 - \epsilon}{d p \epsilon^3} \cdot \frac{\epsilon_r^3 d p_r}{1 - \epsilon_r} \quad (8)$$

The boundary conditions (see Stanek and Szekely, 1974, and Szekely and Poveromo, 1975) required for the solution of Equation (8) are given below:

$$\psi = 0 \quad \text{at} \quad r = 0 \quad (9)$$

$$\psi = -0.5 \quad \text{at} \quad r = 1 \quad (10)$$

$$\frac{\partial \psi}{\partial z} = 0 \quad \text{at} \quad z = 0 \quad \text{and} \quad z = 1 \quad (11a, b)$$

Equations (9) and (10) constitute the statement of cylindrical symmetry and the imperviousness of the walls, respectively, while Equations (11a) and (11b) were deduced from experimental measurements of Szekely and Poveromo (1975) which indicated that the pressure field was laterally uniform both at the exit and at the inlet.

The Component Balance

Following Bird (1960), for steady state conditions and for an isothermal system, the balance on component A takes the form

$$\nabla \cdot \epsilon \rho_A' \vec{v}' = \nabla \cdot [\epsilon D \rho' \cdot \nabla y_A'] + (1 - \epsilon) r_A' \quad (12)$$

where \vec{v}' denotes the interstitial velocity.

Upon recalling the axial, cylindrical symmetry, and defining

$$\epsilon \rho' v_r' = G_r', \quad \epsilon \rho' v_z' = G_z', \quad \text{and} \quad y_A' = \rho_A' / \rho' \quad (13)$$

we may put Equation (12) in the form

$$\frac{1}{r'} \frac{\partial}{\partial r'} (r' G_r' y_A') + \frac{\partial}{\partial z'} (G_z' y_A') = \frac{1}{r'} \frac{\partial}{\partial r'} \left[r' \epsilon \rho' D_r \frac{\partial y_A'}{\partial r'} \right] + \frac{\partial}{\partial z'} \left[\epsilon \rho' D_z \frac{\partial y_A'}{\partial z'} \right] + (1 - \epsilon) r_A' \quad (14)$$

where D_r and D_z are the radial and the axial dispersion coefficients, respectively.

The boundary conditions for Equation (14) are given as follows:

$$r' = 0, \quad \frac{\partial y_A'}{\partial r'} = 0 \quad (15)$$

$$r' = R, \quad \frac{\partial y_A'}{\partial r'} = 0 \quad (16)$$

$$z' = 0, \quad G_z' (y_A' - y_{A_f}') = \rho' D_z \epsilon \frac{\partial y_A'}{\partial z'} \quad (17)$$

$$z' = L, \quad \frac{\partial y_A'}{\partial z'} = 0 \quad (18)$$

Here, Equations (15) and (16) are self explanatory, while Equations (17) and (18) are the so-called Danckwerts

boundary conditions (Danckwerts, 1953).

Upon introducing the following dimensionless variables

$$G_r = G_r'/G_o', \quad G_z = G_z'/G_o', \quad y_A = y_A'/y_{Af}',$$

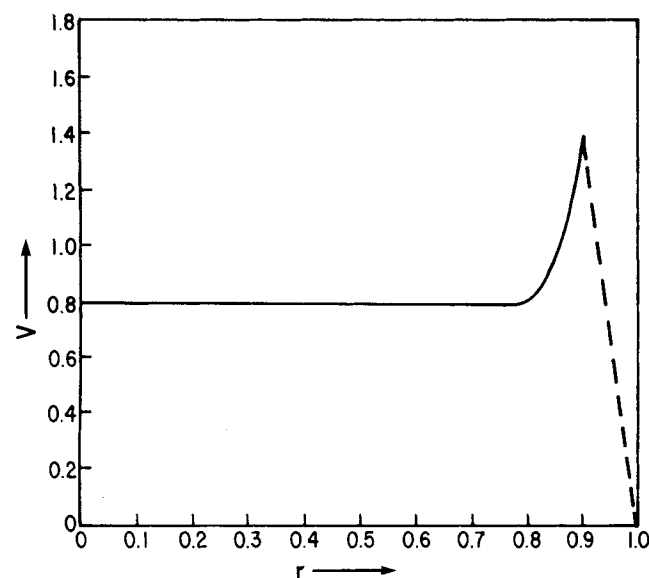
$$\rho = \rho'/\rho_f', \quad r_A = r_A'/r_{Af}' \quad (19)$$

where the subscript *f* denotes feed conditions, and noting that for an incompressible fluid $\rho = 1$, we may write Equation (14) as

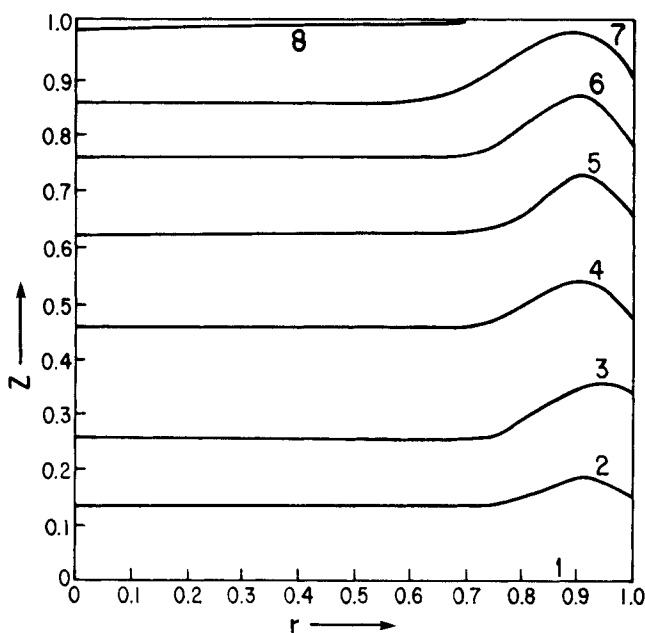
$$G_r \frac{\partial y_A}{\partial r} + a G_z \frac{\partial y_A}{\partial z} = \frac{D_r \rho_f'}{G_o' R} \frac{\partial}{\partial r} \left[r \epsilon \frac{\partial y_A}{\partial r} \right]$$

$$+ \frac{D_z \rho_f'}{G_o' L} a \frac{\partial}{\partial z} \left[\epsilon \frac{\partial y_A}{\partial z} \right] + \epsilon \frac{\partial y_A}{\partial r} \frac{\partial}{\partial r} \left[\frac{D_r \rho_f'}{G_o' R} \right]$$

$$+ a \epsilon \frac{\partial y_A}{\partial z} \frac{\partial}{\partial z} \left[\frac{D_z \rho_f'}{G_o' L} \right] + \frac{(1 - \epsilon) r_{Af}' L}{G_o' y_{Af}'} \cdot a \cdot r_A \quad (20)$$



a. Computed exit velocity profile



b. Computed curves of constant concentrations

Fig. 2. Computed velocity and concentration profiles for uniform packing. a) Computed exit velocity profile, b) computed curves of constant concentrations (curves 1, 2, 3, 4, 5, 6, 7, 8 correspond to $Y_A = 0.997, 0.950, 0.90, 0.85, 0.80, 0.75, 0.70, 0.65$, respectively).

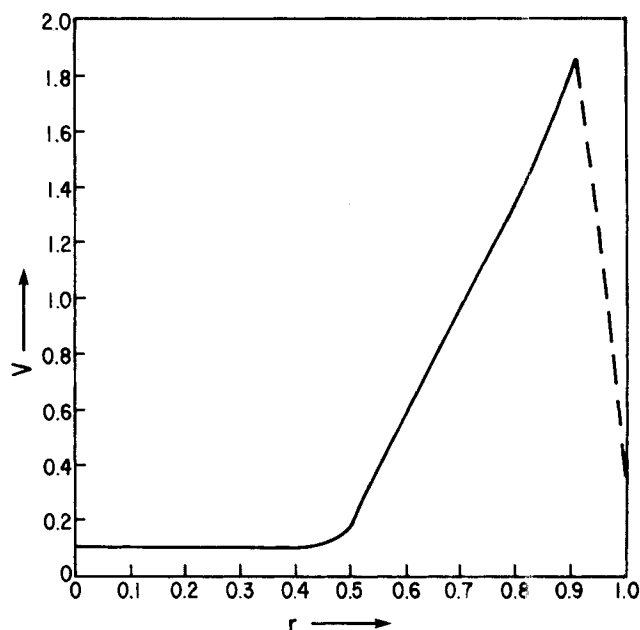


Fig. 3. Computed exit velocity profile for a bed with a high resistance central core.

For a first-order irreversible reaction

$$r_A = -y_A \quad (21)$$

G_o' is the mean superficial mass velocity. We may also write that

$$G_o' = G_{oi}' \epsilon_{av} \quad (22)$$

G_{oi}' is the mean interstitial mass velocity. Written in terms of these quantities, Equation (20) takes the form

$$G_r \frac{\partial y_A}{\partial r} + a G_z \frac{\partial y_A}{\partial z} = \frac{1}{Pe_r} \frac{1}{\epsilon_{av}} \cdot \frac{1}{r} \frac{\partial}{\partial r} \left(\epsilon r \frac{\partial y_A}{\partial r} \right)$$

$$+ \frac{a}{Pe_z} \cdot \frac{1}{\epsilon_{av}} \frac{\partial}{\partial z} \left(\epsilon \frac{\partial y_A}{\partial z} \right) - Da(1 - \epsilon)y_A$$

$$- \frac{\epsilon}{\epsilon_{av}} \frac{\partial y_A}{\partial r} \frac{1}{(Pe_r)^2} \frac{\partial Pe_r}{\partial r} - a \frac{\epsilon}{\epsilon_{av}} \frac{\partial y_A}{\partial z} \frac{1}{(Pe_z)^2} \frac{\partial Pe_z}{\partial z} \quad (23)$$

TABLE 1. PROPERTY VALUES USED IN THE COMPUTATION

1) Uniform bed

$$\frac{dp}{R} = 0.0527$$

$$\epsilon = 0.44$$

$$Re = 4.0$$

$$Da = 0.0822$$

$$a = R/L = 1/6$$

2) High resistance core

$$\frac{dp_2}{R} = 0.025$$

$$\frac{dp_1}{R} = 0.10$$

$$Re = 200.0$$

$$\epsilon_2 = \epsilon_1 = 0.40$$

$$\epsilon_I = 0.288$$

$$\epsilon_w = 0.504$$

$$a = 1/5$$

- i) $Da = 0.10$
ii) $Da = 2.0$

(3) High resistance annulus

$$\frac{dp_2}{R} = 0.10$$

$$\frac{dp_1}{R} = 0.025$$

$$Re = 200.0$$

$$\epsilon_2 = \epsilon_1 = 0.40$$

$$\epsilon_I = 0.288$$

$$\epsilon_w = \epsilon_1$$

$$a = 1/5$$

- i) $Da = 0.10$
ii) $Da = 2.0$

where Pe_z and Pe_r are the axial and the radial Peclet numbers, respectively, and Da is the Damkohler number.

For most practical cases, $(Pe_z)^2$ and $(Pe_r)^2$ will be large; therefore, the last two terms on the right-hand side of Equation (23) may be neglected. Thus we have

$$\frac{1}{Pe_r} \frac{\epsilon}{\epsilon_{av}} \frac{\partial^2 y_A}{\partial r^2} + \left[\frac{\epsilon}{\epsilon_{av}} \cdot \frac{1}{r} \frac{1}{Pe_r} + \frac{1}{Pe_r \epsilon_{av}} \frac{\partial \epsilon}{\partial r} - G_r \right] \frac{\partial y_A}{\partial r} + \frac{a}{Pe_z} \frac{\epsilon}{\epsilon_{av}} \frac{\partial^2 y_A}{\partial z^2} + a \left[\frac{1}{Pe_z} \frac{1}{\epsilon_{av}} \frac{\partial \epsilon}{\partial z} - G_z \right] \frac{\partial y_A}{\partial z} - Da(1 - \epsilon)y_A = 0 \quad (24)$$

The boundary conditions [Equations (15) to (18)] are

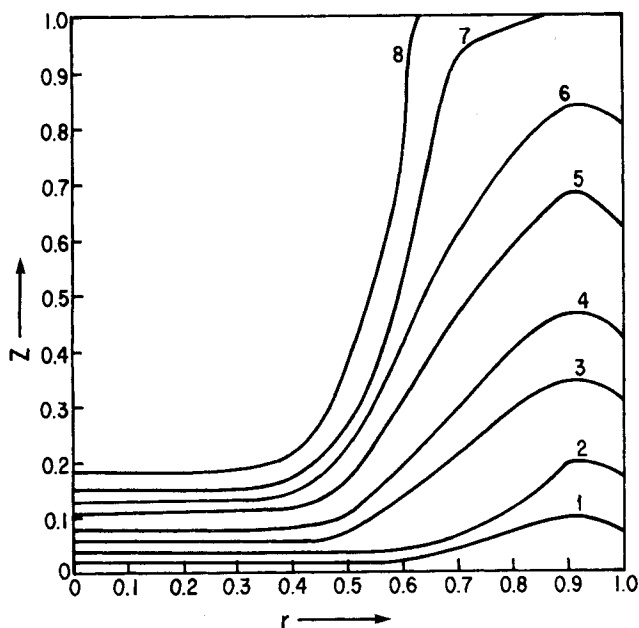
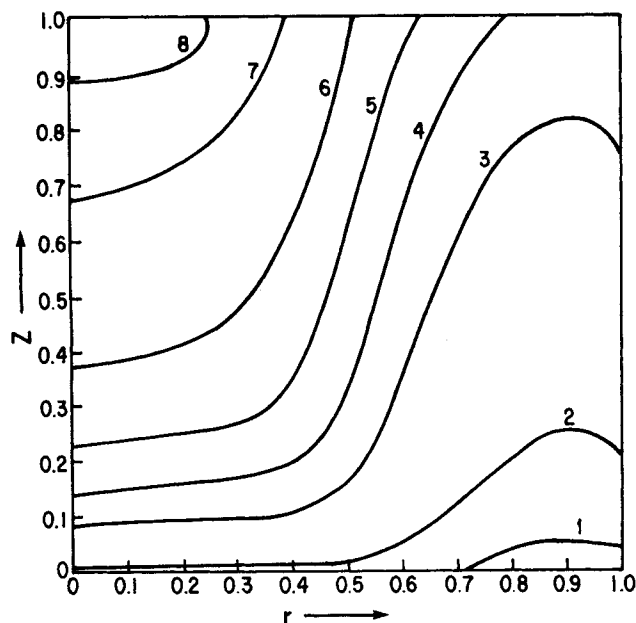


Fig. 4. Computed curves of constant concentration for a bed with a high resistance central core. a) Constant concentration curves for $Da = 0.10$ (curves 1, 2, 3, 4, 5, 6, 7, 8 correspond to $Y_A = 0.99, 0.95, 0.80, 0.70, 0.60, 0.50, 0.40, 0.35$, respectively), b) constant concentration curves for $Da = 2.0$ (curves 1, 2, 3, 4, 5, 6, 7, 8 correspond to $Y_A = 0.7, 0.5, 0.3, 0.2, 0.1, 0.06, 0.04, 0.02$, respectively).

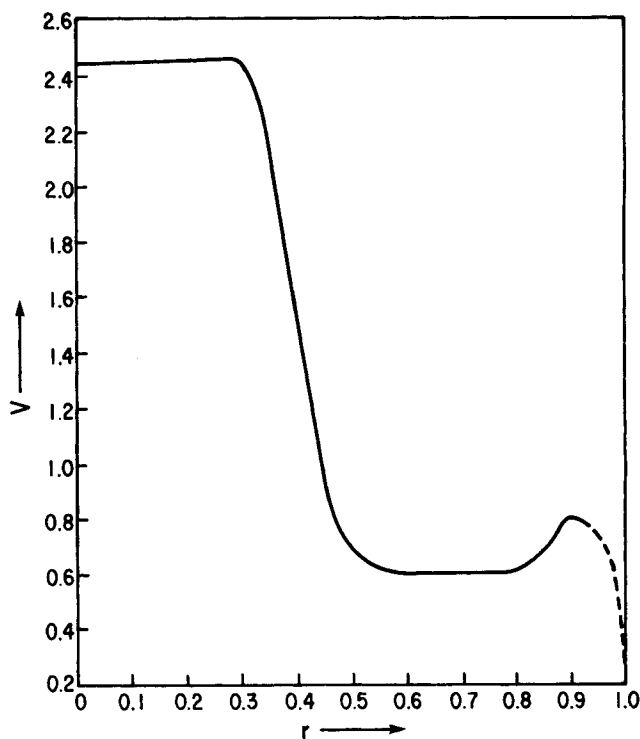


Fig. 5. Computed exit velocity profile for a bed with a high resistance annulus.

readily transcribed in a dimensionless form but are not reproduced here.

Equations (7) and (24) together with their associated boundary conditions represent the complete statement of the problem. These equations have to be solved numerically.

COMPUTED RESULTS

Both the stream Equation (7) and the component balance Equation (24) are elliptic; as customary, these equations were solved using successive underrelaxation. An 11×21 computational grid was used, and finite-difference expressions (using second-order central difference formulas) were used for unequal spacing in the r and the z directions. The value of relaxation parameter used for the flow equation was 0.85, and the number of iterations varied from 30 to 70. For the mass transfer equation, the relaxation parameter was found to be between 0.2 and 0.35, and the number of iterations was usually in the range of 40 to 80. The computer time required was in the range of 20 to 70 s on the CDC 6400 of State University of New York at Buffalo. In order to check the accuracy of the computational scheme, a limiting case of very high Peclet numbers ($Pe_r = Pe_z = 1000$) was taken, and the computed concentrations were compared with the values obtained analytically by assuming a plug flow behavior. These two sets of results agreed to within 1%. Details of the computational scheme are available in the thesis (Choudhary, 1976) on which this work is based.

The packing configurations investigated are sketched in Figure 1, and the property values used in the computation are summarized in Table 1. These quantities were so selected as to represent the conditions employed in the experimental study to be described in Part II.

The following comments may be appropriate regarding the parameters chosen for the computation.

1. The Peclet numbers appearing in Equation (24)

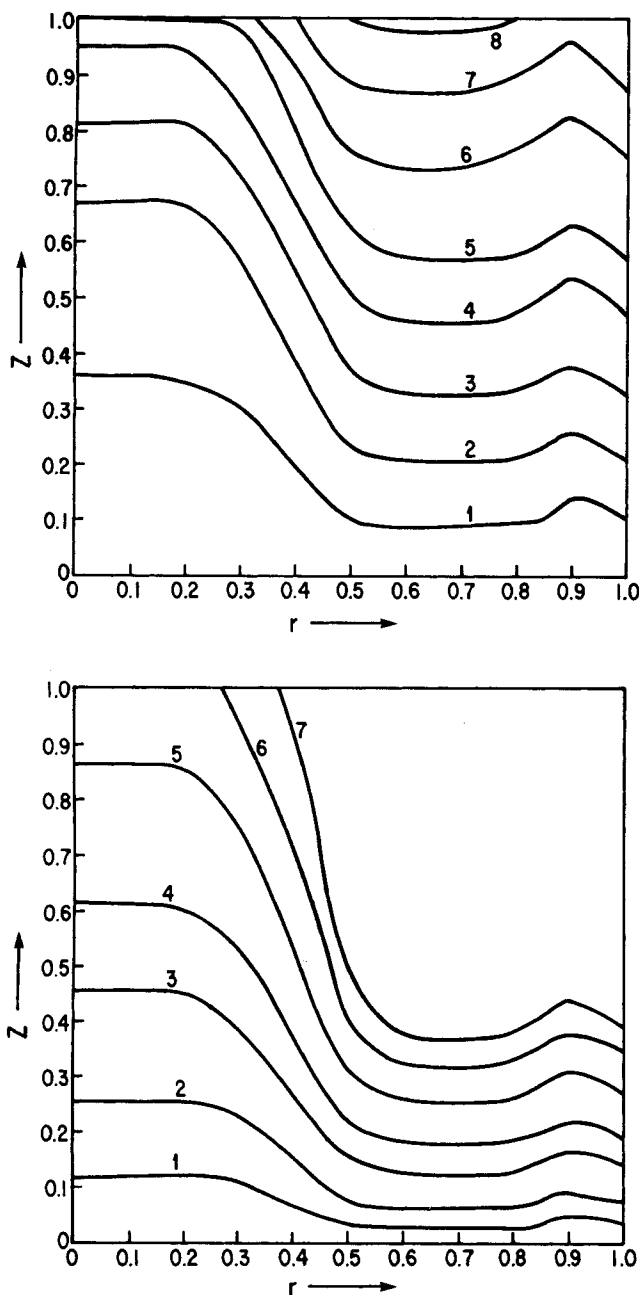


Fig. 6. Computed curves of constant concentration for a bed with a high resistance annulus. a) Constant concentration curves for $Da = 0.10$ (curves 1, 2, 3, 4, 5, 6, 7, 8 correspond to $Y_A = 0.95, 0.90, 0.85, 0.80, 0.75, 0.70, 0.65, 0.60$, respectively), b) constant concentration curves for $Da = 2.0$ (curves 1, 2, 3, 4, 5, 6, 7 correspond to $Y_A = 0.70, 0.50, 0.30, 0.20, 0.10, 0.06, 0.04$, respectively).

were approximated by the following expressions:

$$Pe_z = 2(L/dp) \quad (25)$$

and

$$Pe_r = 10(R/dp) \quad (26)$$

2. An approximate allowance was made for the higher porosity near the wall by adjusting the porosity at the grid point adjacent to the wall in accordance with measurements reported by Benenati and Brosilow (1962). The flow resistance ascribed to the grid point at the wall was infinity to ensure the no-slip condition.

3. An approximate allowance was made for local decrease in the porosity at the interface separating the regions composed of particles having different sizes, through the use of Furnas's (1929) correlation.

4. The particles were assumed to be spherical, and the packing was considered to be random.

Figure 2 shows a plot of the computed velocity profile at the exit together with the concentration isopleths, drawn for a uniformly packed bed.

It is seen that both the velocity and the concentration profiles are flat, except for the region close to the walls, where the preferential flow is readily apparent. The isopleths are consistent with the velocity field, indicating a lower local conversion near the walls.

Figure 3 shows the exit velocity profile for the case where the central core has a higher resistance to flow than the surrounding annular space; the resultant flow maldistribution is readily apparent.

Figure 4 shows the concentration isopleths, corresponding to the velocity profile given in Figure 3, for moderate and fast reaction rates, as expressed by the Damkohler number.

The marked distortion of the concentration isopleths as caused by the flow maldistribution is readily noted on both these plots.

Figure 5 shows the velocity profile obtained for the system where the high resistance zone is located in the annular region. The corresponding concentration isopleths are plotted in Figures 6a and b for moderate and for high reaction rates, respectively. Here, again, the distortion of the concentration isopleths, as caused by the flow maldistribution, is readily apparent. It is noted, moreover, that packing arrangement with a high resistance annular region compensates (in fact, overcompensates in the present case) for the preferential flow near the wall.

NOTATION

- a = R/L (aspect ratio) $^{-1}$
- dp = particle diameter
- dp_r = reference particle size
- D, D_r, D_z = mass diffusivity vector, its components
- Da = $\frac{r_{Af}'R}{G_{oi}'y_{Af}}$, Damkohler number
- f_1 = $\frac{150\mu(1-\epsilon)^2}{dp^2\epsilon^3}$, parameter of resistance
- f_2 = $\frac{1.75\rho'(1-\epsilon)}{dp\epsilon^3}$, parameter of resistance
- f_{2r} = resistance parameter calculated for reference values of dp and ϵ
- f_{20} = dimensionless parameter of resistance
- G_{oi}' = mean interstitial mass velocity
- G_r', G_z' = radial and axial superficial mass velocity components
- G_r, G_z = dimensionless superficial mass velocity components
- L = length of the reactor
- P' = pressure
- Pe_r = $\frac{RG_{oi}'}{\rho_f'D_r}$, radial Peclet number
- Pe_z = $\frac{LG_{oi}'}{\rho_f'D_z}$, axial Peclet number
- r', r = dimensional, dimensionless radial coordinate
- r_A', r_A = dimensional, dimensionless rate of reaction
- R = radius of the reactor
- Re = $\frac{V_o'dp\rho'}{\mu}$, Reynolds number
- v', v_r', v_z' = interstitial velocity vector, its components
- V', V' = superficial velocity vector, its magnitude

\vec{V}_0' = mean superficial velocity
 V, V_r, V_z = dimensionless superficial velocity, its components
 y_A', y_A = mass fraction of A, mass fraction of A normalized with feed concentration
 z', z = dimensional, dimensionless axial coordinate

Greek Letters

ϵ = void fraction
 μ = dynamic viscosity
 ψ = dimensionless stream function
 ξ = ratio of viscous and turbulent resistance parameters
 ρ', ρ = dimensional, dimensionless density
 ρ_A' = mass concentration of A

LITERATURE CITED

- Benenati, R. F., and C. B. Brosilow, "Void Fraction Distribution in Beds of Spheres," *AIChE J.*, **8**, 359 (1962).
 Bird, R. B., W. E. Stewart, and E. N. Lightfoot, *Transport Phenomena*, Wiley, New York (1960).
 Choudhary, M. K., "Effect of Flow Maldistribution on Conversion in a Catalytic Packed Bed Reactor," M.S. thesis, State Univ. N. Y., Buffalo (1976).
 Danckwerts, P. V., "Continuous Flow Systems, Distribution of Residence Times," *Chem. Eng. Sci.*, **2**, 1 (1953).
 Ergun, S., "Fluid Flow Through Packed Columns," *Chem. Eng. Progr.*, **48**, 89 (1952).
 Furnas, C. C., "Flow of Gases Through Beds of Broken Solids," *Bull.* 307, U.S. Bureau of Mines (1929).
 Jaffe, S. B., "Hot Spot Simulation in Commercial Hydrogenation Processes," *Ind. Eng. Chem. Process Design Develop.* (1976).
 Radestock, J., "Theoretische Untersuchung der Stationaeren Inkompressiblen und Kompressiblen Stroemung in Ruhenden, Geschichteten und Isotropen Schuettungen," Dissertation, Fakultat fur Bergbau, Huetttenwesen und Maschinenwesen der Technischen Universitaet Clausthal (1969).
 ———, and R. Jeschar, "Ueber die Stroemung durch die Hochofenschuettung," *Stahl und Eisen*, **22**, 1249 (1970).
 ———, "Theoretische Untersuchung der Inkompressiblen und Kompressiblen Stroemung durch Reaktor-Schuettungen," *Chem. Ing. Tech.*, **43**, 355 (1971a).
 ———, "Theoretische Untersuchung der Gegenseitigen Beeinflussung von Temperatur und Stroemungsfeldern in Schuettungen," *ibid.*, **43**, 1304 (1971b).
 Stanek, V., and J. Szekely, "The Effect of Non-uniform Porosity in Causing Flow Maldistributions in Isothermal Packed Beds," *Can. J. Chem. Eng.*, **50**, 9 (1972).
 ———, "Flow Maldistribution in Two-Dimensional Packed Beds Part II: The Behaviour of Non-Isothermal Systems," *ibid.*, **51**, 22 (1973).
 ———, "Three-Dimensional Flow of Fluids Through Non-uniform Packed Beds," *AIChE J.*, **20**, 974 (1974).
 Szekely, J., and J. Poveromo, "Flow Maldistribution in Packed Beds: A Comparison of Measurement with Predictions," *ibid.*, **21**, 769 (1975).
 Manuscript received April 22, 1976; revision received July 20, and accepted July 21, 1976.

Part II. Experimental Studies

MANOJ CHOUDHARY
 SOL W. WELLER
 and
 JULIAN SZEKELY

Department of Chemical Engineering
 State University of New York at Buffalo
 Buffalo, New York 14214

The modeling equations formulated for a catalytic packed-bed reactor with distributed resistance to flow have been applied to the alumina catalyzed isomerization of 1-butene to cis- and trans-2-butene. Flow maldistribution was deliberately created in a 5.25 cm I.D. reactor by packing different radial sections with alumina particles of different size. Effluent gas composition, monitored by gas chromatography, was found to vary with radial position in a manner consistent with the modeling equations and with the reaction rate constant previously established in a microreactor.

SCOPE

Problems associated with maldistributed flow through a catalytic packed-bed reactor are of major importance in determining the efficiency and life of the catalytic reactor. Modeling equations describing point conversion as a function of position in a reactor having distributed resistance to flow were developed in Part I. The present paper is an experimental study to verify the extent of validity of these equations in model systems. The double-bond isomerization of 1-butene over alumina was chosen as the model reaction for study. The reaction has the advantages of following first-order kinetics, being essentially thermo-neutral, and showing stable activity at 200°C over an extended period of time. The rate constant for the reac-

tion with the particular alumina studied (a Davison product) was first established independently in a flow microreactor system. The fractional conversion of 1-butene, as a function of radial position in the effluent stream, was then followed in a 5.25 cm I.D. reactor for four packing configurations: uniformly sized large particles throughout, uniformly sized small particles throughout, small particles in the central core and large particles in the outer annulus, and large particles in the central core and small particles in the outer annulus. Temperatures in the catalyst bed were monitored by thermocouples at various axial stations, both at the center of the bed and at the wall. Composition of the gas leaving the bed, as a function of radial position, was monitored with a small, movable probe which led directly to a gas chromatograph. Good resolution of all the butene isomers was obtained.

Manoj Choudhary and Julian Szekely are with the Department of Materials Science and Engineering, Massachusetts Institute of Technology, Cambridge, Massachusetts 02139.